Spectroscopic and Magnetic Properties of FeOCl Intercalated with Organosulfur Electron Donors

S. M. Kauzlarich,[†⊥] J. F. Ellena,[‡] P. D. Stupik,[§] W. M. Reiff,[§] and B. A. Averill*[‡]

Contribution from the Department of Chemistry, Michigan State University, East Lansing, Michigan 48824, the Department of Chemistry, University of Virginia, Charlottesville, Virginia 22901, and the Department of Chemistry, Northeastern University, Boston, Massachusetts 02115. *Received September 10, 1986*

Abstract: In an effort to develop a new type of low-dimensional conductor, the intercalation chemistry of FeOCl with tetrathiolene molecules has been explored. New intercalation compounds of the organic electron donors TTF (tetrathiafulvalene), TMTTF (tetramethyltetrathiafulvalene), TTN (tetrathianaphthalene), and TTT (tetrathiatetracene) with the inorganic host FeOCl were prepared by direct reaction of solutions of the organosulfur compounds with solid FeOCl. The new phases obtained were $FeOCl(TTF)_{1/8.5}$, $FeOCl(TMTTF)_{1/13}$, $FeOCl(TTN)_{1/9}(tol)_{1/22}$, and $FeOCl(TTT)_{1/9}(tol)_{1/23}$. X-ray powder diffraction data are consistent with the tetrathiolene molecule being oriented perpendicular to the layers, with the exception of $FeOCl(TMTTF)_{1/13}$, in which the TMTTF molecule is oriented parallel to the host layers. Detailed wideline ^1H and cross polarization magic angle spinning (CPMAS) ^{13}C NMR studies carried out on $FeOCl(TTF)_{1/8.5}$ and related model compounds indicate that there is more than one type of ordering of the TTF molecules characterized by different average TTF environments and/or dynamics. The pressed powder electrical conductivity of FeOCl intercalated with these tetrathiolenes is 10^3-10^5 times that of the pristine material ($\sigma_{RT}FeOCl \sim 10^{-7}$ $(\Omega\text{-cm})^{-1}$). The temperature dependence of the conductivity is consistent with FeOCl and the intercalates being semiconductors with apparent bandgaps of 0.6 eV and ca. 0.3-0.4 eV, respectively. Infrared spectra indicate that the tetrathiolene molecules exist as radical cations within the layers. Mössbauer spectra are consistent with reduction of 4-6% of the Fe^{3+} in FeOCl to Fe^{2+} upon intercalation.

The traditional view that solid-state systems are an area of interest primarily to physicists has changed rapidly within the past 20 years. Chemists are actively investigating the synthesis and properties of solid-state low-dimensional conductive materials.[1] The activity in this field was initially stimulated by the hypothesis that a one-dimensional organic compound could be designed that would exhibit room temperature superconductivity.[2] The discovery of the organic metal TTF-TCNQ (tetrathiafulvalene-tetracyanoquinodimethane) provided further stimulus. Its high conductivity[3] ($\sigma_{RT} \sim 1000$ $(\Omega\text{-cm})^{-1}$) is attributed to the presence of segregated stacks of donor (TTF) and acceptor (TCNQ) molecules and to the occurrence of partial charge transfer between the two.[4-6] Compounds of this general type that crystallize as *mixed* stacks are usually insulators. Although a great deal of interest in organic metals has stemmed from their technological potential, their application has been limited due to the fragility of the crystals as well as the difficulties in synthesis.

Synthetic strategies under investigation in other laboratories include the use of selenium and tellurium analogues of organic donors, more complex π systems, a variety of inorganic anions, and electrochemical synthesis. All of these strategies have had some success.[5,6] The use of the selenium analogue of the organic electron donor TMTTF (tetramethyl)tetrathiafulvalene) provided the first organic superconductor at ambient pressure, $(TMTSF)_2ClO_4$ (TMTSF = tetramethyltetraselenafulvalene).[7] The most recent additions to the class of organic superconductors are based on bis(ethylenedithiolotetrathiafulvalene) (BEDTTTF, referred to as ET): e.g., $(ET)_2ReO_4$,[7] $(ET)_2I_3$,[8] $(ET)_2IBr_2$,[9] and $(ET)_2AuI_2$.[10] The ET charge-transfer compounds lack the columnar stacking that is the most prominent feature in $(TMTSF)_2ClO_4$ and other organic metals.[4-6] Instead, they contain a two-dimensional network in which the interstack S-S contact distances are less than the sum of the van der Waals radii.[1f,4-6,8-10] In addition to the the structural considerations, a nonintegral oxidation state of the donor (and/or acceptor) is also necessary in order to achieve high conductivity in these materials.[1,3-9]

A desire to enforce the formation of segregated stacks of radical cations derived from electron donors led to consideration of intercalation chemistry as a general route to new low-dimensional materials.[11] Intercalation, in its simplest conception, can be viewed as the insertion of a species into a layered matrix by expansion of one crystallographic axis; the identity of both the guest and host species is preserved. The structure of FeOCl is shown in Figure 1a. The layers are held together by van der Waals interactions, which accounts for the fact that molecules can be

[†] Michigan State University.
[‡] University of Virginia.
[§] Northeastern University.
[⊥] Current address: Department of Chemistry, University of California, Davis, Davis, CA 95616.

(1) (a) *Physics and Chemistry of Low-Dimensional Solids*; Alcacēr, L., Ed.; D. Reidel Press: Dordrecht, Holland, 1980. (b) Miller, J. S.; Epstein, A. J. *Prog. Inorg. Chem.* **1976**, *20*, 1-151. (c) Day, P. *Chem. Br.* **1983**, *19*, 306-310. (d) Hoffman, B. M.; Ibers, J. A. *Acc. Chem. Res.* **1983**, *16*, 15-21. (e) Greene, R. L.; Street, G. B. *Science (Washington, DC)* **1984**, *226*, 651-656. (f) Williams, J. M.; Carneiro, K. *Advances Inorg. Chem. Radiochem.* **1985**, *29*, 249-296.

(2) (a) Little, W. A. *Sci. Am.* **1965**, *212*, 21-27. (b) Little, W. A. *Phys. Rev.* **1964**, *134A*, 1416-1424.

(3) (a) Ferraris, J.; Cowan, D. O.; Walatka, V., Jr.; Perlstein, J. H. *J. Am. Chem. Soc.* **1973**, *95*, 948-949. (b) Coleman, L. B.; Cohen, M. J.; Sandman, D. J.; Yamagishi, F. G.; Garito, A. F.; Heeger, A. J. *Solid State Commun.* **1973**, *12*, 1125-1132.

(4) (a) Bechgaard, K.; Andersen, J. R. In *Physics and Chemistry of Low-Dimensional Solids*; Alcacēr, L., Ed.; D. Reidel Press: Dordrecht, Holland, 1980; pp 247-263. (b) Torrance, J. B. *Acc. Chem. Res.* **1979**, *12*, 79-86. (c) Wudl, F. *Acc. Chem. Res.* **1984**, *17*, 227-232.

(5) Khidekel, M. L.; Zhilyaeva, E. I. *Synth. Met.* **1981**, *4*, 1-34.

(6) (a) Williams, J. M. *Prog. Inorg. Chem.* **1985**, *33*, 183-220. (b) Williams, J. M.; Beno, M. A.; Wang, H. H.; Leung, P. C. W.; Emge, T. J.; Geiser, U.; Carlson, K. D. *Acc. Chem. Res.* **1985**, *18*, 261-267. (c) Lerstrup, K.; Talham, D.; Bloch, A.; Pochler, T.; Cowan, D. *J. Chem. Soc., Chem. Commun.* **1982**, 336-337. (d) Wudl, F. *Pure Appl. Chem.* **1982**, *54*, 1051-1058. (e) Wudl, F.; Aaron-Shalom, E. *J. Am. Chem. Soc.* **1982**, *104*, 1154-1156. (f) Aharon-Shalom, E.; Becker, J. Y.; Bernstein, J.; Bittner, S.; Shaik, S. *Synth. Met.* **1985**, *11*, 213-220.

(7) (a) Bechgaard, K.; Carneiro, K.; Olsen, M.; Rasmussen, F. B.; Jacobsen, C. S. *Phys. Rev. Lett.* **1981**, *46*, 852-855. (b) Parkin, S. S. P.; Engler, E. M.; Schumaker, R. R.; Lagier, R.; Lee, V. Y.; Scott, J. C.; Greene, R. L. *Phys. Rev. Lett.* **1983**, *50*, 270-273.

(8) (a) Williams, J. M.; Emge, T. J.; Wang, H. H.; Beno, M. A.; Copps, P. T.; Hall, L. N.; Carlson, K. D.; Crabtree, G. W. *Inorg. Chem.* **1984**, *23*, 2558-2560. (b) Crabtree, G. W.; Carlson, K. D.; Hall, L. N.; Copps, P. T.; Wange, H. H.; Emge, T. J.; Beno, M. A.; Williams, J. M. *Phys. Rev. B* **1984**, *30*, 2958-2960.

(9) Williams, J. M.; Wang, H. H.; Beno, M. A.; Emge, T. J.; Sowa, L. M.; Copps, P. T.; Behroozi, F.; Hall, L. N.; Carlson, K. D.; Crabtree, G. W. *Inorg. Chem.* **1984**, *23*, 3839-3841.

(10) Wang, H. H.; Beno, M. A.; Geiser, U.; Firestone, M. A.; Webb, K. S.; Nunez, L.; Crabtree, G. W.; Carlson, K. D.; Williams, J. M.; Azevedo, L. J.; Kwak, J. F.; Schirber, J. E. *Inorg. Chem.* **1985**, *24*, 2465-2466.

(11) Averill, B. A.; Kauzlarich, S. M. *Mol. Cryst. Liq. Cryst.* **1984**, *107*, 55-64.

0002-7863/87/1509-4561$01.50/0

Table I. Chemical Analyses for FeOCl and the $FeOCl(T)_x(S)_y$ Compounds[a]

	T	x	S	y	% C[b]	% H[b]	% Cl[b]	% Fe[b]	% S[b]
FeOCl							33.04	52.05	
							32.47	52.33	
FeOCl	TTF	1/8.5			6.45	0.36	26.99	42.13	11.49
					6.53	0.70	26.07	42.13	11.42
FeOCl	TTF	1/11	tol	1/21	8.10	0.58	27.20	42.84	8.95
					7.47	0.91	27.10	42.46	8.12
FeOCl	TMTTF	1/13			7.26	0.73	27.85	43.87	7.75
					7.32	0.79	27.44	44.13	7.89
FeOCl	TTN	1/9.22	tol	1/22	12.15	0.58	25.53	40.22	10.02
					12.56	0.74	24.83	40.56	10.10
FeOCl	TTT	1/9.5	tol	1/23	17.78	0.87	23.88	37.61	9.09
					14.59	0.81	23.09	37.64	8.74

[a] T = tetrathiolene and S = solvent. [b] Calculated values on the first line and observed values on the second line.

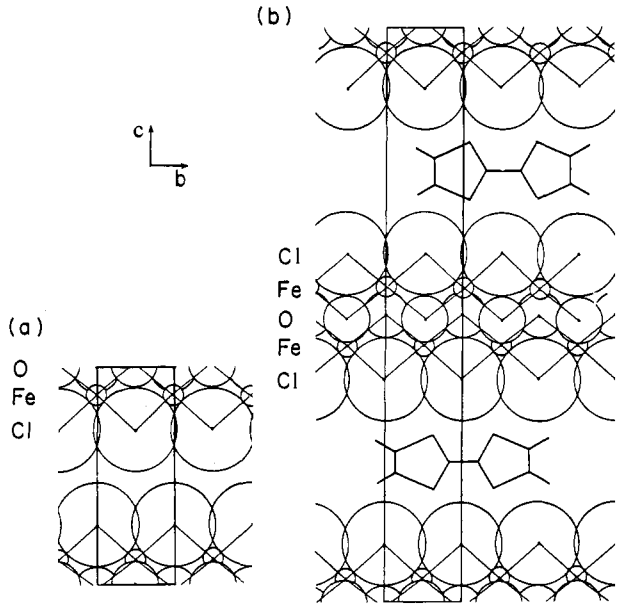

Figure 1. A representation of (a) FeOCl and (b) $FeOCl(TTF)_{1/8.5}$. The unit cell is outlined.

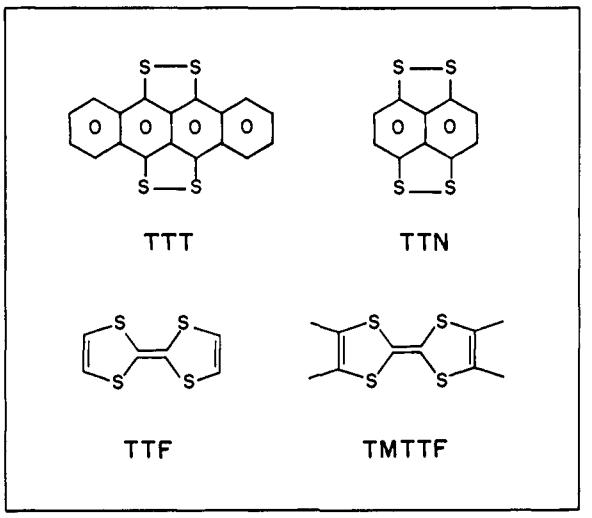

Figure 2. Schematic drawings of the organosulfur molecules intercalated into FeOCl.

easily intercalated into this material. Since intercalation compounds generally adopt stoichiometries approximating close packing of the intercalant molecules,[12] the resulting orbital overlap between intercalants should allow facile charge transfer between adjacent molecules. A wide variety of polar organic compounds as well as organometallic species[13-15] are known to intercalate into FeOCl, resulting in a significant expansion of the interlayer distance and increased conductivity (10^3–10^5) over that of FeOCl ($\sigma_{RT} = 10^{-7}$ $(\Omega\text{-cm})^{-1}$). The intercalation chemistry of FeOCl has been expanded to include TTF[16] and the other tetrathiolene molecules shown in Figure 2. The following new phases have been obtained: $FeOCl(TTF)_{1/8.5}$, $FeOCl(TMTTF)_{1/13}$, $FeOCl(TTN)_{1/9}(tol)_{1/22}$ (TTN = tetrathianaphthalene), and $FeOCl(TTT)_{1/9}(tol)_{1/23}$ (TTT = tetrathiatetracene). A number of physical techniques have been used to obtain information on the properties of these materials, including X-ray powder diffraction and EXAFS (Extended X-Ray Absorption Fine Structure) spectroscopy,[17] infrared and optical spectroscopy, and variable temperature magnetic susceptibility and conductivity[18] studies. In addition, detailed neutron powder diffraction[19] and wideline ^1H and cross polarization magic angle spinning (CPMAS) ^{13}C NMR studies have been performed on $FeOCl(TTF)_{1/8.5}$. Neutron powder diffraction and NMR provide information on the static and dynamic ordering, respectively, of the guest species. These techniques, taken together, have provided insight into the details of the reaction and the properties of the resulting intercalates.

Experimental Section

Materials. Preparation of all intercalates was performed under an argon atmosphere. TTF, obtained from Parish or Aldrich Chemical Co. was recrystallized once from cyclohexane/hexanes.[20] High purity TTF, obtained from Strem Chemical Co., was handled exclusively under inert atmosphere. TMTTF,[21] TTF(CA)[22] (CA = chloranil), and $TTF_3Br_2 \cdot 2H_2O$[23] were prepared by published procedures. TTT, prepared by a published procedure,[24] was purified by Soxhlet extraction[25] and subse-

(12) Gamble, F. R.; Geballe, T. H. *Treatise on Solid State Chemistry*; Hannay, N. B., Ed.; Plenum Press: New York, 1976; Vol. III, pp 89–166.
(13) *Intercalation Chemistry*; Whittingham, M. S., Jacobson, A. J., Ed.; Academic Press: New York, 1982.
(14) Herber, R. H. *Acc. Chem. Res.* **1982**, *15*, 216–224, and references cited therein.
(15) (a) Halbert, T. R.; Scanlon, J. C. *Mater. Res. Bull.* **1979**, *14*, 415–421. (b) Halbert, T. R.; Johnston, D. C.; McCandlish, L. E.; Thompson, A. H.; Scanlon, J. C.; Dumesic, J. A. *Physica* **1980**, *99B*, 128–132. (c) Schäfer-Stahl, H.; Abele, R. *Mat. Res. Bull.* **1980**, *15*, 1157–1165. (d) Schäfer-Stahl, H.; Abele, R. *Angew. Chem., Int. Ed. Engl.* **1980**, *19*, 477–478.
(16) Antonio, M. R.; Averill, B. A. *J. Chem. Soc., Chem. Commun.* **1981**, 382–383.
(17) (a) Kauzlarich, S. M.; Teo, B. K.; Averill, B. A. *Inorg. Chem.* **1986**, *25*, 1209–1215. (b) Kauzlarich, S. M.; Averill, B. A.; Teo, B. K. *Mol. Cryst. Liq. Cryst.* **1984**, *107*, 65–73. (c) Averill, B. A.; Kauzlarich, S. M.; Teo, B. K.; Faber, J., Jr. *Mol. Cryst. Liq. Cryst.* **1985**, *120*, 259–262.
(18) Averill, B. A.; Kauzlarich, S. M.; Antonio, M. R. *J. Phys. (Paris)* **1983**, *44*, 1373–1376.
(19) Kauzlarich, S. M.; Stanton, J.; Faber, J., Jr.; Averill, B. A. *J. Am. Chem. Soc.* **1986**, *108*, 7946–7951.
(20) *Inorganic Syntheses*; Shriver, D. F., Ed.; John Wiley & Sons, Inc.: New York, 1979; Vol. 19, pp 28–34.
(21) Ferraris, J. P.; Poehler, T. O.; Bloch, A. N.; Cowan, D. O. *Tetrahedron Lett.* **1973**, *27*, 2553–2556.
(22) Girlando, A.; Marzola, F.; Pecile, C.; Torrance, J. B. *J. Chem. Phys.* **1983**, *79*, 1075–1085.
(23) Kaplan, M. L.; Wudl, F.; Haddon, R. C.; Hauser, J. J. *Chemica Scripta* **1980**, *15*, 196–202.
(24) (a) Marschalk, C.; Stumm, C. *Bull. Soc. Chim. Fr.* **1948**, *15*, 418–428. (b) Goodings, E. P.; Mitchard, D. A.; Owen, G. *J. Chem. Soc., Perkin Trans. 1* **1972**, 1310–1314.

quently by several sublimations at 210 °C under vacuum. TTN was a gift from B. K. Teo of Bell Laboratories, Murray Hill, NJ. FeOCl was prepared according to a literature procedure.[13,26]

Preparation of Intercalates. FeOCl and the intercalant were weighed and transferred to a Teflon-stoppered reaction flask that contained a Teflon-coated stir bar (10 × 4 mm). Approximately 15–25 mL of an appropriate solvent was added. The reaction mixture was evacuated via the Teflon stopcock and sealed. The flask was wrapped with aluminum foil to ensure protection from the light. It was placed in an oil bath whose temperature was controlled by a variable resistor and had typical fluctuations of ±5 °C. After a period of 1–4 weeks, the reaction flask was removed, and the mixture was transferred to a glass frit. The resulting black microcrystalline solid was washed with freshly distilled solvent and dried acetone under inert atmosphere. The solid was dried at room temperature for 12 h under vacuum. Intercalation was verified by X-ray powder diffraction, mass spectrometry, and elemental analysis (Galbraith Laboratories). Elemental analyses for the intercalates are listed in Table I.

$FeOCl(TTF)_x(tol)_y$. Toluene (25–30 mL) was added to solid FeOCl (100 mg) and TTF (100 mg) (mole ratio (2:1)) to produce a bright yellow solution. This reaction takes a minimum of 1 week at 70 °C. The absorption peaks in the optical spectra of the acetone eluant could be assigned to TTF^+;[26] in addition, a peak at 360 nm was assigned to $FeCl_3$: $1/9 < x < 1/12$, $1/18 < y < 1/25$.

$FeOCl(TTF)_x$. Concentrations (5–7 mM) of intercalant in dimethoxyethane (DME) solution were used in these reactions. The mole ratio of FeOCl to intercalant was 2:1. The reaction took 10 days at 50 °C. The optical spectra of the acetone eluant consisted of absorption peaks due to TTF^+ and a very small amount of $FeCl_3$. No solvent was detectable by mass spectrometry: $1/8 < x < 1/9$.

$FeOCl(TMTTF)_x$. TMTTF is only slightly soluble in MeCN. Therefore, a saturated solution was prepared by dissolving TMTTF in a minimum amount of warm MeCN. This solution was transferred via cannula to the reaction flask. The mole ratio of FeOCl to TMTTF was 2:1. Once in contact with solid FeOCl, the solution gradually turned from yellow-orange to a yellow-green color. The reaction took a minimum of 13 days at 55 °C. Optical spectra of the MeCN eluant indicated the presence of $TMTTF^+$:[24b] $1/13 < x < 1/14$.

$FeOCl(TTN \text{ or } TTT)_x(tol)_y$. Mole ratios (FeOCl/intercalant) were 6:1 and 3:1 for TTN and TTT intercalants, respectively. These compounds are sparingly soluble in only a few solvents such as DMF, hot toluene, and methylene chloride. There was always undissolved intercalant in the reaction mixture, which was heated at 70 °C. The TTN and TTT reactions took 28 and 45 days, respectively. Both reaction products were washed thoroughly (Soxhlet extraction with methylene chloride for 3 days or 8–10 h of continuous washing with toluene). As with the other acetone eluants, the optical spectra could be assigned to the tetrathiolene radical cation.[28] Carbon analyses for the TTT intercalate were irreproducible; that given in Table I is typical: $1/7 < x < 1/9$, $1/19 < y < 1/26$.

NMR Spectra. Proton NMR spectra of solid TTF and $FeOCl(TTF)_{1/8.5}$ were recorded on a Nicolet NT-360 spectrometer. Digitization rates of up to 2 MHz were achieved with a Nicolet 2090 digital oscilloscope. All spectra were obtained at 20 ± 2 °C. Proton spectra (361 MHz) were recorded with a standard Nicolet transmitter and probe. All radio frequency pulses were shortened until spectral line shapes were independent of pulse width; 3.5 μs (45°) pulses were used. Proton ^{13}C cross polarization and magic angle spinning were used to obtain ^{13}C spectra of solids at 37.7 MHz on a Nicolet NT-150 at the Colorado State University Regional NMR Center. In all experiments the delay time between data acquisition and the following pulse was adjusted so that an increase in delay time had no effect on the spectral line shapes. Phase cycling and data routing for echo experiments were performed as described by Bloom et al.[29] and Griffin.[30] During echo experiments, data acquisition was begun before the top of the echo, and points collected prior to the echo peak were removed before Fourier transformation. The only phase correction necessary for echo spectra was that required to correct for misalignment of the transmitter and receiver phases (no first-order correction was used). Flipback pulses[31] were used to accelerate data acquisition in the CPMAS experiments.

Optical and Infrared Spectroscopy. Solid-state spectra of Fluorolube mulls between NaCl or quartz plates were recorded on a Cary 17DI spectrophotometer in transmission mode. Infrared spectra were obtained from KBr pellets on a Perkin-Elmer Model 1430 grating spectrophotometer.

Magnetic Susceptibility and Mössbauer Spectra. Temperature dependent magnetic susceptibilities were measured from 5 to 300 K on a SHE Corporation SQUID susceptometer. Mössbauer spectra were obtained on a conventional constant acceleration spectrometer operated in conjunction with a Canberra Series 35 multichannel analyzer, by using a 100-mCi ^{57}Co in rhodium metal matrix γ-ray source. Temperature control was achieved by using an uncalibrated silicon diode coupled to a Lake Shore Cryotronics Model DT-500 C set point controller. Temperature measurements were made with a digital voltmeter by using a calibrated silicon diode driven by a 10-μA constant current source. Spectra below room temperature were obtained by using either a flow-type or exchange-type Janis cryostat in either a horizontal or vertical mode. Isomer shifts are relative to metallic Fe at room temperature.

Conductivity. Two-probe powder conductivity measurements[32] were performed with a home-built apparatus. All measurements were conducted at room temperature. The samples were 3–4 mm long and were held in a 2-mm diameter precision bore Pyrex cell. The sample could be pressed to a maximum pressure of ca. 800 Pa. The constant voltage source was a homemade D.C. power source capable of supplying 1.3–24 V. Typically 1–5 V were applied to the sample. The current was measured by a Keithley Model 600 electrometer or a Model 177 microvolt digital multimeter. All samples measured obeyed Ohm's law.

Results and Discussion

Synthesis. Intercalation reactions of tetrathiolenes were run with various solvents such as toluene, acetonitrile, and dimethoxyethane. The intercalation reactions of TTN and TTT require longer reaction times (22–45 days) at higher temperature (65–70 °C) than the other intercalants, due to their extremely low solubility in most solvents.

TMTTF is soluble in toluene, methylene chloride, and acetonitrile (sparingly). Due to the initial success of toluene as a solvent for TTF,[16] it was used for the intercalation of TMTTF. Repeated attempts always produced a two-phase system in addition to unreacted FeOCl. Powder X-ray diffraction data showed two low angle peaks corresponding to d = 13.59 and 11.94 Å, in addition to that of the FeOCl (010) reflection, suggestive of two orientations of TMTTF within FeOCl. The observed d-spacings are consistent with TMTTF lying perpendicular (13.59 Å) and parallel (11.94 Å) to the FeOCl layers. A similar phenomenon has been reported to occur with $FeOCl(p\text{-phenylenediamine})_{1/9}$.[33] Intercalation with acetonitrile as solvent provided a one-phase system for $FeOCl(TMTTF)_{1/x}$, in which the plane of the TMTTF molecule is parallel to the host layers.[17a]

Stabilization of the radical cation by dimethoxyethane has been cited as the reason for facile intercalation of metallocenes into FeOCl.[34] Solvents clearly play a role in the intercalation process of the tetrathiolenes. The presence of the radical cation in the reaction mixture indicates that solvation of the radical cation may be important. Further work on the mechanism of these intercalation reactions is in progress.

Structural Studies. X-ray powder diffraction,[17a] EXAFS,[19] and neutron powder diffraction[19] studies on the FeOCl tetrathiolene intercalants have been reported. The proposed structure of $FeOCl(TTF)_{1/8.5}$ is shown in Figure 1b. With the exception of TMTTF, the tetrathiolene molecules are aligned along the *bc* plane and appear to be approximately close packed.

Solid-state NMR spectroscopy has been used to elucidate the orientation of guest species in layered materials.[35] The major

(25) Teo, B. K.; Snyder-Robinson, P. A. *Inorg. Chem.* **1979**, *18*, 1490–1495.
(26) (a) Lind, M. D. *Acta. Crystallogr., Sect. B: Struct. Crystallogr. Cryst. Chem.* **1970**, *B26*, 1058–1062. (b) Kikkawa, S.; Kanamaru, F.; Koizumi, M. *Bull. Chem. Soc. Jpn.* **1979**, *52*, 963–966. (c) Grant, R. W.; Wiedersich, H.; Housley, R. M.; Espinosa, G. P.; Artman, J. O. *Phys. Rev. B* **1971**, *3*, 678–684.
(27) Mayerle, J. J.; Torrance, J. B.; Crowley, J. I. *Acta. Crystallogr., Sect. B: Struct. Crystallogr. Cryst. Chem.* **1979**, *B35*, 2988–2995.
(28) Perez-Albuerne, E. A.; Johnson, H., Jr.; Trevoy, D. J. *J. Chem. Phys.* **1971**, *55*, 1547–1554.
(29) Bloom, M.; Davis, J. H.; Valic, M. I. *Can. J. Phys.* **1980**, *58*, 1510–1517.
(30) Griffin, R. G. *Methods Enzymol.* **1981**, *72*, 108–174.
(31) Tegenfeldt, J.; Haeberlen, U. *J. Mag. Res.* **1979**, *36*, 453–457.
(32) (a) Yemen, M. R., Ph.D. Thesis, Michigan State University, 1983. (b) Dye, J. L. *Prog. Inorg. Chem.* **1984**, *32*, 327–441.
(33) Maeda, Y.; Yamashita, M.; Ohshio, H.; Tsutsumi, N.; Takashima, Y. *Bull. Chem. Soc. Jpn.* **1982**, *55*, 3138–3143.
(34) Schäfer-Stahl, H. *Synth. Met.* **1981**, *4*, 65–69.

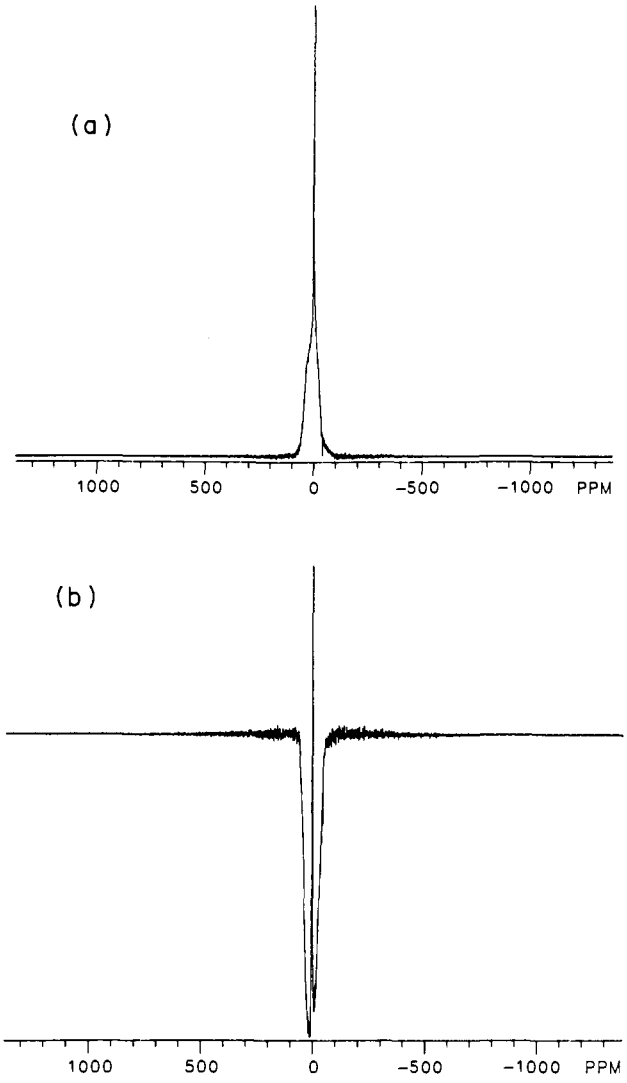

Figure 3. ^{1}H FT NMR spectrum for TTF obtained by employing (a) θ_0–τ–θ_{90} and (b) θ_0–τ–θ_0 pulse sequences.

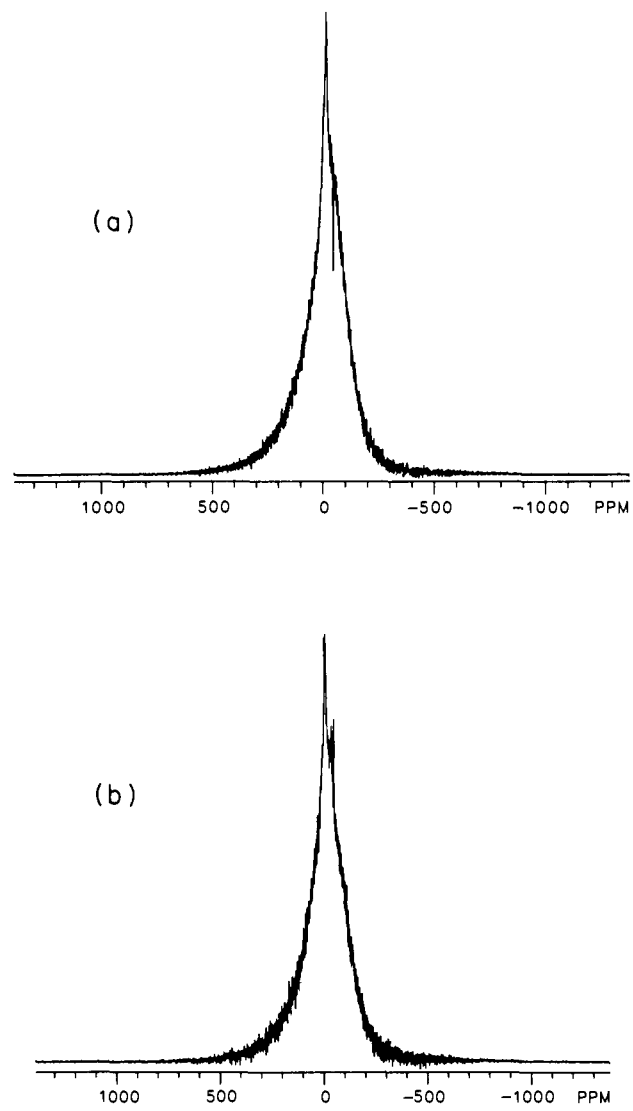

Figure 4. ^{1}H FT NMR spectrum for $FeOCl(TTF)_{1/8.5}$ obtained by (a) θ_0–τ–θ_{90} and (b) θ_0–τ–θ_0 pulse sequences.

obstacle in obtaining undistorted wideline spectra of solids is the slow recovery of the receiver, which produces dead-time. This limitation does not allow one to collect the initial part of the free induction decay (FID), which for very broad line spectra causes substantial distortion of the base line.[36] Also, more rapid digitization than is commonly used in solution FT NMR is needed. The dead-time problem is overcome with use of an echo technique.

The most common pulse sequence used to produce echoes in solids is θ_0–τ–θ_{90}, where θ is the pulse angle (the subscripts indicate the relative phases of the pulse and τ is the time between pulses).[36,37] Since the Nicolet 360-MHz spectrometer at the University of Virginia is not capable of providing 90° pulses that uniformly excite the entire spectral frequency range of interest, pulse times (and therefore angles) were decreased until distortion was minimized. Figure 3a shows the spectrum of solid TTF obtained with a θ_0–τ–θ_{90} sequence.[38] The spectrum obtained following a θ_0–τ–θ_0 sequence is shown in Figure 3b. The spectrum is almost identical with the θ_0–τ–θ_{90} spectrum, except that the broad component is 180° out of phase with respect to the same component of the θ_0–τ–θ_{90} spectrum. This is expected when strong intra- and intermolecular spin 1/2 homonuclear dipole interactions are present.[39]

Table II. Line Widths and Relative Area of Echo ^{1}H Spectra of $FeOCl(TTF)_{1/8.5}$ and of the θ_0–τ–θ_{90} ^{1}H Spectra of TTF

pulse sequence	spctrl compnnt	full line width at half height (kHz)	% of total spctrl area	ratio of θ_0–τ–θ_0:θ_0–τ–θ_{90} spctrl area
θ_0–τ–θ_{90}[a]	sharp	4	3	
	broad	61	97	
θ_0–τ–θ_0[a]	sharp	4	4	
	broad	60	96	
				1.2
θ_0–τ–θ_{90}[b]	sharp	1	16	
	broad	23	84	

[a] $FeOCl(TTF)_{1/8.5}$. [b] TTF.

θ_0–τ–θ_{90} and θ_0–τ–θ_0 ^{1}H spectra of $FeOCl(TTF)_{1/8.5}$ are shown in Figure 4 (parts a and b). These spectra consist of at least two components, shown by a sharp and a broad line. Table II lists

(35) (a) Silbernagel, B. G. *Chem. Phys. Lett.* **1974**, *34*, 298–301. (b) Clough, S.; Palvadeau, P.; Venien, J. P. *J. Phys. C* **1982**, *15*, 641–655. (c) Rouxel, J.; Palvadeau, P. *Rev. Chim. Min.* **1982**, *19*, 317–332. (d) Molitor, M.; Müller-Warmuth, W.; Spiess, H. W.; Schöllhorn, R. *Z. Naturforsch, A: Phys., Phys. Chem., Kosmophys.* **1983**, *38A*, 237–246. (e) Grant, P. M. *Phys. Rev. B* **1982**, *26*, 6888–6895. (f) Röder, U.; Müller-Warmuth, W.; Schöllhorn, R. *J. Chem. Phys.* **1981**, *75*, 412–417. (g) Röder, U.; Müller-Warmuth, W.; Speiss, H. W.; Schöllhorn, R. *J. Chem. Phys.* **1982**, *77*, 4627–4631.

(36) Fukushima, E.; Roeder, S. B. *Experimental Pulse NMR. A Nuts and Bolts Approach*; Addison-Wesley Publishing Co., Inc.: Reading, MS, 1981.

(37) Mansfield, P. *Prog. NMR Spectrosc.* **1971**, *8*, 41.

(38) Experimental parameters for all NMR spectra can be found in the Supplemental Material.

(39) Boden, N.; Levine, Y. K.; Lightowlers, D.; Squires, R. T. *Mol. Phys.* **1975**, *29*, 1877–1891.

the relative intensities and line widths of the two components for both $FeOCl(TTF)_{1/8.5}$ and TTF. The sharp component is at about 1 ppm (relative to Me_4Si in $CDCl_3$) and may be due to mobile TTF or absorbed solvent. Similar ^1H spectra have been observed for pyridine and picolines intercalated into VOCl.[35b] In the case of VOCl, the sharp component was attributed to mobile intercalant molecules at crystal defects. The broad component of the $FeOCl(TTF)_{1/8.5}$ echo spectra is considerably broader than its counterpart in the TTF spectrum and appears to be a single Gaussian line. This indicates that the magnetic interactions that determine line width in $FeOCl(TTF)_{1/8.5}$ and TTF are quite different. Assuming that the TTF molecules in $FeOCl(TTF)_{1/8.5}$ are at best closest-packed, the rigid lattice second moment was calculated by using Van Vleck's formula.[40] To calculate the second moment, the chloride ions of FeOCl were assumed to be 100% ^{35}Cl and the shortest H--Cl distance to be 2.3 Å. The calculated second moment can then be used in eq 1 to obtain the

$$\Delta H_1 = 2.35(\Delta H^2)^{1/2} \quad (1)$$

width of the resonance line at half maximum height in units of G. Equation 1 is valid assuming that the second moment is not dominated by a single nuclear pair interaction. This appears to be the case for the broad component in the $FeOCl(TTF)_{1/8.5}$ ^1H echo spectrum. The experimental line width (60 kHz) is considerably greater than that calculated (ΔH_1 = 29.9 kHz) considering only H--H and H--Cl interactions, indicating that other strong magnetic interactions are important. It has been determined in the ^1H NMR study of pyridine and picolines intercalated into VOCl that dipolar interactions between the protons and the unpaired spin density on the chloride ions provide a large contribution to the line widths at high magnetic field (4.7 T).[35b] A similar situation is expected for $FeOCl(TTF)_{1/8.5}$. Line broadening due to the presence of unpaired spin density on the protons (hyperfine exchange broadening) of the radical cation of TTF would be small compared to the dipolar mechanism.[41] Broadening by the dipolar mechanism will contribute to inhomogeneous lines, while the hyperfine mechanism will contribute to homogeneous lines.

In order to learn more about the interactions causing the line broadening in the $FeOCl(TTF)_{1/8.5}$ spectra, a series of hole-burning experiments were performed. In these experiments, a portion of the spectrum was irradiated with a continuous radio frequency field, and then the entire spectrum was recorded (Figure 5). Field strengths ($\gamma B_2/2\pi$) of 145 and 43 Hz were applied during the delay between the end of the acquisition and the echo pulse sequence for the spectra. Figure 5 shows the spectra obtained by using a field strength of 43 Hz. Irradiation of a portion of the spectrum prior to the observation pulses clearly changes the spectral line shape. This indicates that the lines are inhomogeneous and that dipolar interactions are important in determining the line width. It should be noted that the relatively small fields which were used for preirradiation affected a rather large spectral width. This may be due to magnetization transfer by molecular motion or spin diffusion. The discontinuities evident in the spectra at large distances from the preirradiation frequency (i.e., 140 and −140 ppm in Figure 5b) indicate that more than one broad spectral component is present, and the preirradiation has different effects on the component amplitudes. The presence of multiple broad components is most simply interpreted as evidence for molecular domains with different structural and/or dynamic characteristics.

Although ^{13}C–^1H CPMAS spectra were obtained for TTF, TTF(CA) salts (both the segregated (ss) and mixed stack (ms) structures),[22] and for $TTF_3Br_2{\cdot}2H_2O$,[43] no ^{13}C spectrum could be observed for $FeOCl(TTF)_{1/8.5}$ under either of the following conditions: (1) CPMAS with high power ^1H decoupling and (2) direct excitation of carbons with MAS and ^1H decoupling. The

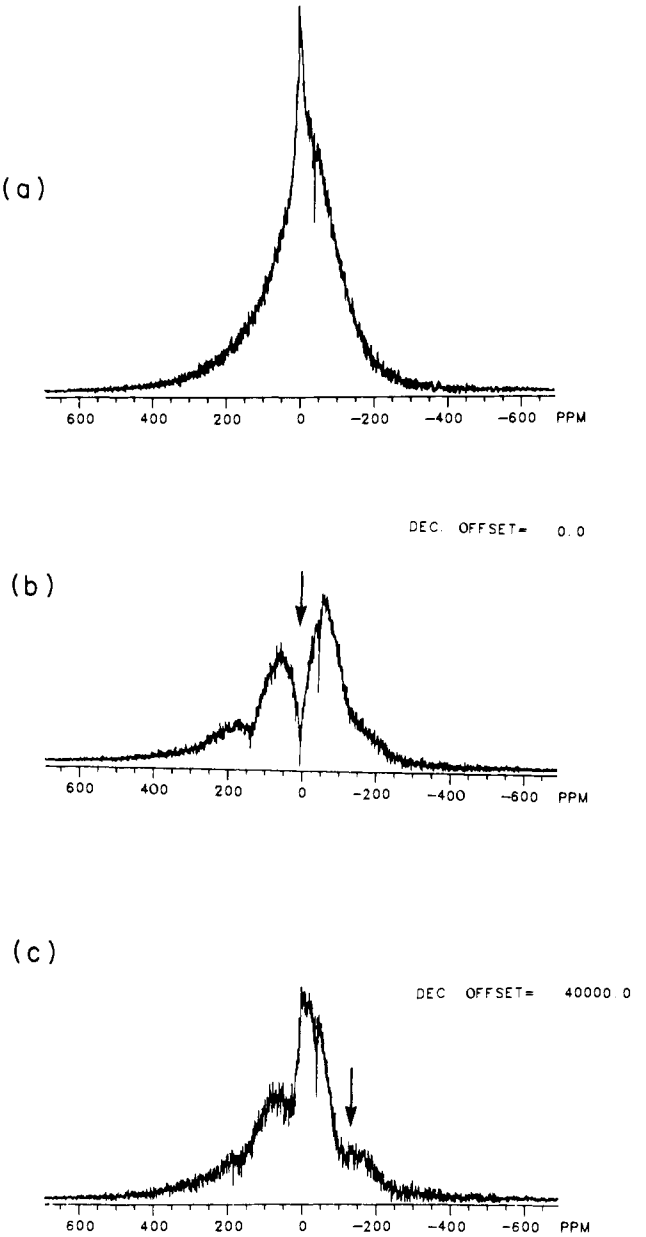

Figure 5. ^1H FT NMR for $FeOCl(TTF)_{1/8.5}$ (a) drawn to the same scale as (b) and (c); (b and c) hole-burning experiments using a field strength of 43 Hz. Arrows indicate location of preirradiation.

fact that no spectrum was observed indicates the presence of strong magnetic interactions that are not present in the simple TTF salts used as models. Just as the chloride–proton interactions appear to have a large effect on the line width of the $FeOCl(TTF)_{1/8.5}$ ^1H spectrum, chloride unpaired spin density–^{13}C nuclear dipolar interactions probably cause the ^{13}C CPMAS spectrum to be too broad to observe. The electronic configuration of the TTF molecule in $FeOCl(TTF)_{1/8.5}$ is expected to be similar to that of TTF(CA) (ss) and $TTF_3Br_2{\cdot}2H_2O$, based on the IR data.[17c] In contrast to $FeOCl(TTF)_{1/8.5}$, the latter salts yield high resolution ^{13}C CPMAS NMR spectra, suggesting that the electronic structure of TTF in $FeOCl(TTF)_{1/8.5}$ is probably not responsible for the severe line broadening.

Infrared Spectroscopy. Extensive molecular vibration studies of charge-transfer compounds with TTF,[44] TMTTF,[45] and TTT[46]

(40) Van Vleck, J. H. *Phys. Rev.* **1948**, *74*, 1168–1183.
(41) Swift, T. J. In *NMR of Paramagnetic Molecules*; LaMar, G. N., Horrocks, W., Jr., Holm, R. H., Eds.; Academic Press: New York, 1973; Chapter 2.
(42) Bramwell, F. B.; Haddon, R. C.; Wudl, F.; Kaplan, M. L.; Marshall, J. H. *J. Am. Chem. Soc.* **1978**, *100*, 4612–4614.
(43) Kauzlarich, S. M.; Ellena, J.; Averill, B. A., unpublished research.
(44) Bozio, R.; Zanon, I.; Girlando, A.; Pecile, C. *J. Chem. Phys.* **1979**, *71*, 2282–2293.
(45) Meneghetti, M.; Bozio, R.; Zanon, I.; Pecile, C.; Ricotta, C.; Zanetti, M. *J. Chem. Phys.* **1984**, *80*, 6210–6224.
(46) (a) Torrance, J. B.; Scott, B. A.; Welber, B.; Kaufman, F. B.; Seiden, P. E. *Phys. Rev. B* **1979**, *19*, 730–741. (b) Kachapina, L. M.; Kaplunov, M. G.; Yagubskii, E. B.; Borod'ko, Yu. G. *Chem. Phys. Lett.* **1978**, *58*, 394–398.

Table III. Correlation of the Position of the $a_g\nu_3$ Band Observed in the Raman Spectrum with the Extent of Charge Transfer[c]

compound	$a_g\nu_3$	charge transfer[a]
TTF^0	1518	0
TTF-TCNQ	1456	0.63
$TTF(I)_{0.71}$	1452	0.67
$TTF(Br)_{0.76}$	1448	0.71
$TTF(Cl)_{0.80}$	1441	0.79
TTF^+	1420	1.00
$FeOCl(TTF)_{1/9}(tol)_{1/21}$	1404	1.00[b]

[a] Reference 49. [b] Reference 65. [c] Frequency in wave numbers.

as the electron donor molecules have been reported. There has been very little work on TTN salts, presumably due to the difficulties in the synthesis of TTN.[47,48] The infrared spectrum of pristine FeOCl shows only a single strong vibrational band at 485 cm^{-1}, which is assigned to the Fe–O stretch.[17c] Consequently, direct information on the guest species can be obtained by infrared spectroscopy. For one-dimensional organic metals, vibrational spectroscopy provides evidence for partial charge transfer if the electronic transition does not introduce too much background absorption. The infrared spectrum for a compound having localized electronic charge distribution would exhibit frequencies of both neutral and ionized molecules, whereas delocalized distributions would be characterized by single frequencies of average values.[49] Radicals participating in strong intermolecular interactions exhibit new vibronic absorptions in the infrared which are due to a mechanism of intensity borrowing from the charge-transfer transition.[44]

In order to assign the infrared spectra of $FeOCl(TTF)_{1/8.5}$, $FeOCl(TTF\text{-}d_4)_{1/9}$ and $FeOCl(TTF)_{1/9}(tol)_{1/22}$, salts of TTF with chloranil, TTF(CA), were prepared, and the vibrational spectra were confirmed.[49] The a_g modes are the only ones allowed by symmetry to couple with the HOMO of TTF^+, resulting in electron–intramolecular vibrational modes.[22] The $a_g\nu_3$ mode consists of the simultaneous stretching of the C=C bonds.[50] It is this vibration that has been used to designate the degree of charge transfer, usually for the Raman data. The $a_g\nu_3$ modes in the Raman spectra of the salts $TTF(I)_{0.71}$, $TTF(Br)_{0.76}$, and $TTF(Cl)_{0.80}$, which exhibit partial charge transfer,[49] and for $FeOCl(TTF)_{1/9}(tol)_{1/21}$[51] are listed in Table III. Linear dependence of vibrational frequencies vs. charge transfer should not be assumed for all organic charge-transfer compounds, but the experimental values obtained for the TTF salts are in approximate agreement with a linear correlation. From the values listed in Table III, it is clear that the TTF moiety in $FeOCl(TTF)_{1/9}(tol)_{1/21}$ is present as the radical cation. Raman spectroscopy is preferred to infrared for determining the extent of charge transfer, since the spectrum obtained is generally simpler and dominated by totally symmetric modes. Infrared spectra are complicated by low-lying electronic absorptions[52] and interference effects.[53]

Complete characterization of both the neutral and fully ionic TTF molecule[50] by infrared spectroscopy has overcome the complexities in the analysis of the infrared data. Information on the degree of charge transfer can be ascertained from the infrared data, which complement the Raman data. The infrared data for $FeOCl(TTF)_{1/8.5}$ and $FeOCl(TTF\text{-}d_4)_{1/9}$ intercalates and for TTF(CA) and $TTF\text{-}d_4$(CA) segregated stack structures[22] are given in Table IV. The frequencies corresponding to CA vibrations have been omitted. Comparison of the spectra of the TTF and $TTF\text{-}d_4$ intercalates shows that these molecules are fully ionic radical cations. The strong infrared absorption at 1340 cm^{-1} has been assigned to the $a_g\nu_3$ mode, based on the comparison of the infrared spectrum of $FeOCl(TTF)_{1/8.5}$ and $FeOCl(TTF\text{-}d_4)_{1/9}$ with that of the CA salt (ss).[17c,22] The strong intensity and the red shift of the $a_g\nu_3$ mode relative to the Raman mode in TTF charge-transfer salts has been predicted by a theoretical model[53a] applied to dimerized segregated stack systems.[44] The intensity of the $a_g\nu_3$ mode observed in the infrared spectrum of $FeOCl(TTF)_{1/9}(tol)_{1/22}$[51] suggests that charge-transfer interactions between TTF radical cations are important for both the toluene and the DME preparation.

$FeOCl(TMTTF)_{1/13}$ exhibits very weak vibrational bands due to the intercalant compared with the Fe–O stretch at 485 cm^{-1}, and the background absorption is much greater than that observed for $FeOCl(TTF)_{1/8.5}$. The infrared data for $FeOCl(TMTTF)_{1/13}$ can be compared to those obtained for $TMTTF^+$ in $(TMTTF)_2X$ where X = Br^- and ClO_4^-[45] (Table V). All the strong peaks observed for $(TMTTF)_2Br$ and $(TMTTF)_2ClO_4$ are also observed for $FeOCl(TMTTF)_{1/13}$, except for the $a_g\nu_3$ band (1361 cm^{-1}), which is absent. The strong intensity of this band in $(TMTTF)_2X$ compounds is attributed to the presence of dimeric units.[45,54] One would expect this mode to be relatively weak in $FeOCl(TMTTF)_{1/13}$, because the TMTTF molecule lies parallel to the FeOCl layers, prohibiting formation of dimers.

The infrared data for $FeOCl(TTT)_{1/9}(tol)_{1/23}$ are listed in Table VI and compared with values for TTT^+ in TTT(X), where X = Cl^-, Br^-, I^-, and SCN^-.[28] With some samples of the TTT intercalate, certain peaks could be assigned to neutral TTT: these may be due to the presence of small amounts of unintercalated TTT on the surface of the intercalate. Otherwise, the data correspond to those of the TTT cation.

Infrared data for TTN salts have not been reported. The only salt whose synthesis has been published to date (TTN·TCNQ) is metallic and thus has no discernable infrared spectrum.[48,55] Infrared data for $FeOCl(TTN)_{1/9}(tol)_{1/21}$ are listed in Table VII and compared with those of the neutral compound. Most of the peaks are red-shifted with respect to the neutral intercalant, as are those of the other intercalants, and may be assigned to the radical cation.

The broad absorption (4000–1600 cm^{-1}) observed in the infrared spectra of $FeOCl(TTF)_{1/8.5}$[17c] is present in the spectra of all the intercalates and appears to be due to an electronic transition. Organic charge-transfer compounds with pressed powder conductivities on the order of 10^{-4}–10^{-2} $(\Omega\text{-cm})^{-1}$ exhibit a similar broad absorbance in this region of the spectrum (4000–1600 cm^{-1}), which has been attributed to the continuum of electronic transitions.[56]

Infrared spectroscopy of the intercalants is consistent with the guest species being fully ionic. The broad IR absorption at about 0.6–0.3 eV is similar to that observed in all the mixed valence compounds of TTF which are conductors[47] and suggests that the intercalates should exhibit an increase in conductivity over that of FeOCl. Although the steric interactions of TMTTF are different from the TTF intercalant, the electronic structure deduced from the infrared data is consistent with TMTTF also being a fully ionic cation. Similar conclusions can be drawn for the TTN and the TTT intercalates. Essentially complete charge transfer from the guest to the host lattice has occurred.

Optical Spectra. The optical spectra of the intercalates are shown in Figure 6. The value of the band gap reported for FeOCl is 1.9 eV,[57] which corresponds to a "break" in the absorption curve.[58] The intercalates have a greater absorption at low energy

(47) Riga, J.; Verbist, J. J.; Wudl, F.; Kruger, A. *J. Chem. Phys.* **1978**, *69*, 3221–3231.
(48) Wudl, F.; Schafer, D. E.; Miller, B. *J. Am. Chem. Soc.* **1976**, *98*, 252–254.
(49) Bozio, R.; Pecile, C. In *Physics and Chemistry of Low-Dimensional Solids*; Alcacér, L., Ed.; Reidel: Dordrecht, Holland, 1980; pp 165–186.
(50) Bozio, R.; Girlando, A.; Pecile, D. *Chem. Phys. Lett.* **1977**, *52*, 503–508.
(51) Antonio, M. R., Ph.D. Thesis, Michigan State University, 1983.
(52) Torrance, J. B. In *Chemistry and Physics of One-Dimensional Metals*; Keller, H., Ed.; Plenum Press: New York, 1977; pp 137–166.
(53) (a) Rice, M. J. *Phys. Rev. Lett.* **1976**, *37*, 36–39. (b) Krâl, K. *Chem. Phys.* **1977**, *23*, 237–242.
(54) Bozio, R.; Meneghetti, M.; Pecile, C. *J. Chem. Phys.* **1982**, *76*, 5785–5795.
(55) Wudl, F., private communication.
(56) Wheland, R. C.; Gillson, J. L. *J. Am. Chem. Soc.* **1976**, *98*, 3916–3925.
(57) Kanamaru, F.; Shimada, M.; Koizumi, M.; Takano, M.; Takada, T. *J. Solid State Chem.* **1973**, *7*, 297–299.
(58) Brec, R.; Schleich, D.; Louisey, A.; Rouxel, J. *Ann. Chim. Fr.* **1978**, *3*, 347–352.

Table IV. Infrared Spectral Features of $FeOCl(TTF)_{1/8.5}$, $FeOCl(TTF\text{-}d_4)_{1/9}$, and the TTF, TTF-$d_4$ Infrared Absorptions of TTF(CA)(ss) and TTF-d_4(CA)(ss)[c]

$FeOCl(TTF)_{1/9}(tol)_{1/21}$[a]	$FeOCl(TTF)_{1/8.5}$	$FeOCl(TTF\text{-}d_4)_{1/9}$	TTF(CA)	TTF-d_4(CA)[b]	assignment[b]
			482 (m)		$a_g\nu_6$
			629 (w)		$b_{2u}\nu_{26}$
684 (s)	695 (m)	525 (w)	700 (w)	540 (w)	$b_{3u}\nu_{34}$
			710 (w)		
		740 (mw)		740 (mw)	$b_{2u}\nu_{25}$
745 (m)	760 (m)		752 (mw)		$b_{1u}\nu_{17}$
820 (m)	835 (mw)		830 (w)	795 (w)	$b_{1u}\nu_{16}$
1080 (w)		830 (mw)	1105 (mw)	832 (mw)	$b_{1u}\nu_{15}$
1250 (w)	1262 (w)		1258 (w)		$b_{2u}\nu_{23}$
1332 (s)	1340 (s)	1335 (s)	1364 (s)	1370 (s)	$a_g\nu_3$
1465 (w)	1478 (m)	1428 (w)	1469 (sh, s)	1432 (sh, s)	$b_{1u}\nu_{14}$
	3070 (w)	2269 (w)	3052 (m)	2268 (m)	$b_{2u}\nu_{22}$
3070 (vw)	3090 (w)	2310 (w)	3070 (m)	2310 (w)	$b_{1u}\nu_{13}$

[a] Reference 51. [b] Reference 22. [c] Frequencies are in cm^{-1}; relative intensities are indicated in parentheses: vs = very strong, s = strong, m = medium, w = weak.

Table V. Infrared Spectral Features for $FeOCl(TMTTF)_{1/13}$ and the TMTTF Infrared Absorptions of $(TMTTF)_2Br$[c]

$FeOCl(TMTTF)_{1/13}$	$(TMTTF)_2Br$[a]	assignment[a]
690 (m)		
940 (m)	935 (ms)	β CH_3
1332 (m)	1340 (vs)	$a_g\nu_4$
	1361 (s)	$a_g\nu_3$
1470 (m)	1438 (mw)	α CH_3 asymm
1560 (m)	1560 (s)	$b_{1u}\nu_{28}$ ($a_g\nu_3$)
2920 (vw)	2923 (w)	ν CH_3 asymm
2960 (vw)	2973 (w)	

[a] Reference 45, some vibrations for $(TMTTF)_2Br$ are not listed. Assignments are as indicated; the methyl group vibrations: α CH_3, H-C-H bending; β CH_3, C-C-H bending; ν CH_3, C-H stretching. [c] Frequencies are in wave numbers; relative intensities are indicated in parentheses: vs = very strong, s = strong, m = medium, w = weak.

Table VI. Infrared Spectral Features for $FeOCl(TTT)_{1/9}(tol)_{1/23}$ and the Infrared Absorptions of TTT(X), X = Cl^-, Br^-, and SCN^-, and TTT^0[b]

$FeOCl(TTT)_{1/9}(tol)_{1/23}$	TTT^+[a]	TTT^0
683 (s)		685 (w)
738 (m)		733 (vs)
752 (m)	751 (m)	742 (s)
761 (m)		
949 (w)		
973 (m)	972 (m)	968 (m)
998 (m)	998 (vs)	
1008 (m)		1010 (w)
1059 (m)	1058 (s)	
1167 (m)	1163 (m)	1148 (w)
1273 (w)	1274 (vs)	1248 (w)
1284 (s)	1286 (vs)	
1311 (s)	1313 (s)	1305 (vs)
1361 (m)	1361 (s)	1319 (s)
1429 (m)	1432 (m)	
1452 (m)		
1463 (s)	1463 (s)	
1504 (w)	1504 (w)	1522 (w)
1552 (m)	1550 (m)	
1598 (m)	1599 (m)	1612 (m)

[a] Reference 28; principal vibrational bands of the four salts were essentially identical. [b] Frequencies are in wave numbers; relative intensities are indicated in parentheses: vs = very strong, s = strong, m = medium, w = weak.

(0.5 eV) and more structure in their spectra at high energy (3.5–1.5 eV) compared to FeOCl.

$FeOCl(TTF)_{1/8.5}$ exhibits a broad absorption centered at about 1200 nm (1.03 eV) (Figure 6). A possibly related transition is observed in the spectra of TTF^+ dimers at 714 nm (1.73 eV).[46a] This corresponds to charge transfer within the $(TTF^+)_2$ dimers as illustrated below.[44,59] For mixed valence salts, there is an additional, stronger charge-transfer band, which is located at

$$(TTF^+)(TTF^+) \rightarrow TTF^0TTF^{2+} \quad (2)$$

Table VII. Infrared Spectral Features for $FeOCl(TTN)_{1/9}(tol)_{1/22}$ and the Infrared Absorptions of TTN^0[a]

$FeOCl(TTN)_{1/9}$-$(tol)_{1/22}$	TTN^0	$FeOCl(TTN)_{1/9}$-$(tol)_{1/22}$	TTN^0
623 (m)	623 (s)		1200 (w)
695 (m)	670 (m)	1260 (m)	1260 (s)
740 (s)	725 (w)	1280 (m)	1280 (s)
810 (s)	797 (s)	1388 (s)	1362 (s)
962 (w)	815 (w)		1370 (s)
975 (w)	965 (w)	1495 (w)	1455 (s)
1100 (w)	1070 (m)	1570 (w)	1540 (s)
1185 (m)	1185 (s)		

[a] Frequencies are in wave numbers; relative intensities are listed in parentheses: vs = very strong, s = strong, m = medium, w = weak.

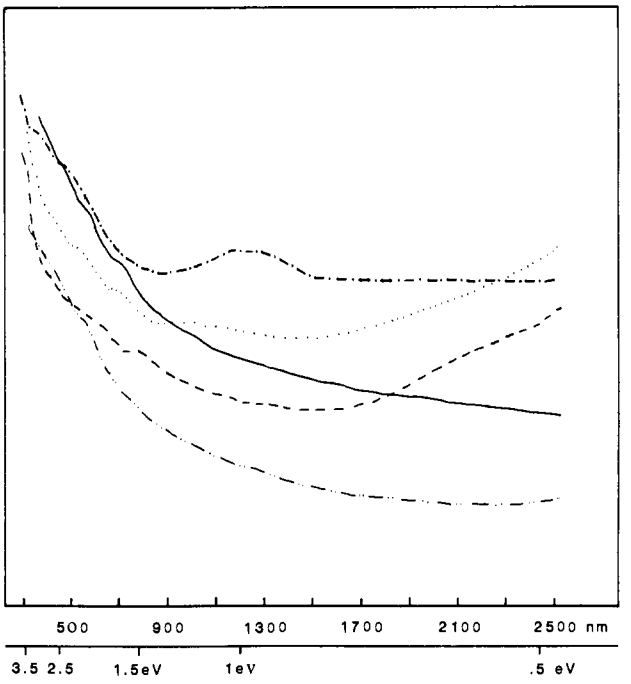

Figure 6. Optical spectra (Flurolube mulls between NaCl plates) for FeOCl (-···-··), $FeOCl(TTF)_{1/8.5}$ (-·-), $FeOCl(TMTTF)_{1/13}$ (—), $FeOCl(TTN)_{1/9}(tol)_{1/21}$ (···), and $FeOCl(TTT)_{1/9}(tol)_{1/23}$ (– – –). The ordinate is an arbitrary absorption scale.

~2000 nm (0.6 eV) for $TTF(Br)_{0.71}$ and $TTF(SCN)_{0.57}$[46,59] corresponding to the transition shown below. For the absorption

$$(TTF)^+(TTF)^0 \rightarrow (TTF)^0(TTF)^+ \quad (3)$$

in $FeOCl(TTF)_{1/8.5}$ centered at 1200 nm, the mechanism of charge

(59) Sugano, T.; Yakushi, F.; Kuroda, H. *Bull. Chem. Soc. Jpn.* **1978**, *51*, 1041–1046.

Table VIII. Two-Probe Pressed Powder Conductivity Measurements for FeOCl and the Intercalates

compound	E_g[a] (eV)	σ_{RT} $(\Omega\text{-cm})^{-1}$
FeOCl	0.61	2.0×10^{-7}
$FeOCl(TTF)_{1/9}(tol)_{1/21}$	0.36	3.5×10^{-3}
$FeOCl(TTF)_{1/8.5}$	0.45	7.8×10^{-4}
$FeOCl(TMTTF)_{1/13}$		1.6×10^{-2}
$FeOCl(TTN)_{1/9}(tol)_{1/22}$	0.35	2.1×10^{-3}
$FeOCl(TTT)_{1/9}(tol)_{1/23}$	0.38	2.3×10^{-3}

[a] From ref 18.

Table IX. Isomer Shift and Quadrupole Splitting for FeOCl, $FeOCl(TTF)_{1/8.5}$, and $FeOCl(TTN)_{1/9}$ at 300 K

compound	IS (mm/s)	QS (mm/s)
FeOCl	0.38	0.92
$FeOCl(TTF)_{1/8.5}$	0.46	0.75
$FeOCl(TTN)_{1/9}$	0.42	0.78

transfer shown in (3) is unlikely due to the absence of evidence for partial charge transfer in the infrared data. The interpretation of this band is uncertain, and data on single crystals of $FeOCl(TTF)_{1/8.5}$ are necessary to determine its origin.

The existence of intervalence charge transfer ($Fe^{3+} \rightarrow Fe^{2+}$) has been proposed based on the evidence from Mössbauer spectroscopy for charge transfer between the guest and host.[60] Most intervalence bands are broad, intense absorptions.[61] The low intensity and poor resolution of these spectra (Figure 6) are similar to those observed for the layered compound $FePS_3$ and its intercalates.[62] Because of the underlying absorption present in these spectra, an intervalence charge-transfer band could not be discerned.

Conductivity. The conductivity obtained from a "single crystal" of $FeOCl(TTF)_{1/8.5}$ was of the same order of magnitude as the powder samples,[18] indicating that the "crystal" was probably an aggregate. High quality single crystals of the intercalates have not yet been obtained by the reaction procedure described. This has made it necessary to measure pressed powder conductivities. The pressed powder conductivity increases from ca. 10^{-7} for pristine FeOCl to ca. 10^{-2} for $FeOCl(TMTTF)_{1/13}$ (Table VIII). $FeOCl(TMTTF)_{1/13}$ exhibits the highest room temperature conductivity, suggesting that the electronic conductivity is due to charge transport within the host lattice rather than to the stacked guest radical cations within the gallery. It has been shown that to obtain high conductivity of the type seen in the organic metals the electron donor molecules must be stacked; this requirement is obviously not met in the TMTTF intercalate in which the plane of the tetrathiolene is parallel to the FeOCl layers.

Mössbauer Spectroscopy. The Mössbauer effect was used to investigate the charge transfer, and dynamics thereof, between host and guest molecules in intercalation compounds of FeOCl. Compounds of this type have been studied by Herber[14,64] and Fatseas et al.[63a] among others. A summary of their results shows that the effects of this charge transfer are as follows: (i) a larger isomer shift in the intercalated compounds than in pristine FeOCl; (ii) an unusual temperature dependence of the quadrupole splitting of the intercalate compared to that of the pure host material; (iii) the appearance of a distinct Fe^{2+} site at low temperatures. The two compounds investigated in detail were $FeOCl(TTF)_{1/8.5}$ and $FeOCl(TTN)_{1/9}$.

Isomer Shift and Quadrupole Splitting. The room temperature Mössbauer parameters of the compounds studied are given in Table IX. The observed increase of the isomer shift upon intercalation in our systems is comparable to that found in the previous reports.[64] This behavior has been explained in terms

Table X. Temperature Dependence of the Quadrupole Splitting for $FeOCl(TTN)_{1/9}$, $FeOCl(TTF)_{1/8.5}$, and FeOCl

sample	T (K)	QS (mm/s)
$FeOCl(TTN)_{1/9}$	298	0.78
	179	1.04
	104	1.50
$FeOCl(TTF)_{1/8.5}$	298	0.75
	179	0.95
	104	1.31
FeOCl	298	0.92
	111	0.97
	94	0.96

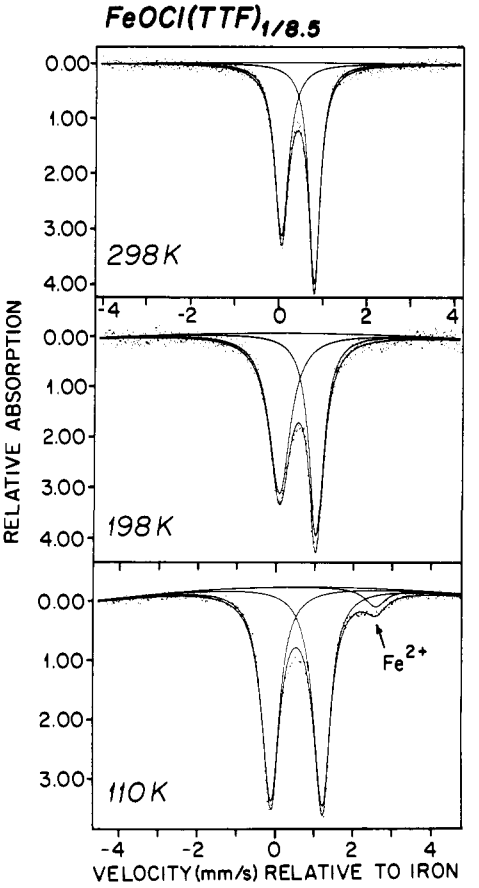

Figure 7. Mössbauer spectra of $FeOCl(TTF)_{1/8.5}$ at various temperatures, with computer-generated fits to the data using two (298 and 198 K) or three (110 K) Lorentzian lines and illustrating the appearance of the Fe^{2+} feature at low temperature.

of a reduction of the host lattice by the guest molecules, in which extra electrons are delocalized within the band structure of the host matrix. A time-averaged spectrum is seen, which reflects a mixed-valence state where the isomer shift is between that of a ferric and ferrous site.

The unusually large temperature dependence of the quadrupole splitting of this class of compound was also observed in our systems as shown in Table X. This behavior is quite different from that of pristine FeOCl, where the quadrupole splitting is relatively temperature independent. This is typical of the ^6A ground state of high-spin iron(III), for which there can be no temperature dependent valence shell occupation contribution to the electric field gradient tensor.

Upon examining the temperature dependence of the Mössbauer spectra, one sees that the positive velocity component of the quadrupole split doublet is of greater intensity than the other at high temperatures, whereas at low temperature the reverse is true. This does not occur for pure unintercalated FeOCl, for which the ratio of the two absorption peaks remains constant with tem-

(60) Eckert, H.; Herber, R. H. *J. Chem. Phys.* **1984**, *80*, 4526-4540.
(61) Allen, G. C.; Hush, N. S. *Prog. Inorg. Chem.* **1967**, *8*, 357-444.
(62) Clément, R.; Garnier, O.; Mathey, Y. *Nouv. J. Chim.* **1982**, *6*, 13-17.
(63) (a) Fatseas, G. A.; Palvadeau, P.; Venien, J. P. *J. Solid State Chem.* **1984**, *51*, 17-37. (b) Meyer, H.; Weiss, A. *Mat. Res. Bull.* **1978**, *13*, 913-922. (c) Schäfer-Stahl, H. *Mat. Res. Bull.* **1982**, *17*, 1437-1446.
(64) Herber, R. H.; Eckert, H. *Phys. Rev. B* **1985**, *31*, 34-41.

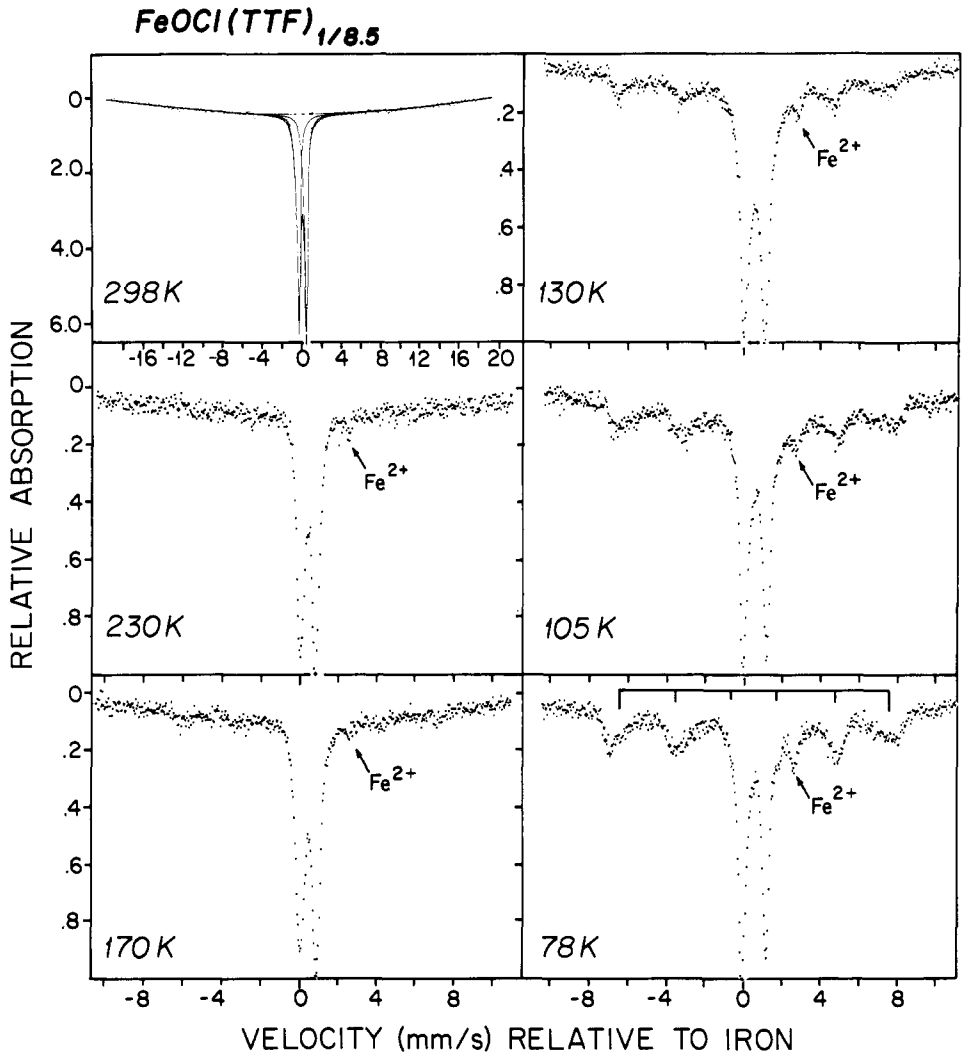

Figure 8. Mössbauer spectra of $FeOCl(TTF)_{1/8.5}$ at various temperatures, illustrating the gradual appearance of a magnetic hyperfine pattern with decreasing temperature.

perature. This phenomenon is shown in Figure 7 for $FeOCl(TTF)_{1/8.5}$ and can be accounted for, at least in part, by the temperature-dependent appearance of the lower velocity component of the ferrous doublet at approximately the same energy as the lower velocity component of the ferric doublet.

The fraction of Fe(II) was approximated by doubling the area under the resonance maximum at 2.6 mm/s and then subtracting this same area from the more intense ferric doublet. $FeOCl(TTN)_{1/9}$ and $FeOCl(TTF)_{1/8.5}$ were found to contain ca. 6.3% and 4% Fe(II) by this method, respectively. These fractions are of the same magnitude as the previously studied nitrogen-containing intercalates.

The above results indicate that the dynamics of the electron-transfer process in these organosulfur intercalates are, in many respects, similar to those found for the nitrogen-containing compounds studied by other groups.[63a,64]

One feature of the present systems that is clearly different, however, is the appearance of the hyperfine background pattern at a significantly higher temperature than is observed for the nitrogen intercalates.[14,64] That is, for the previously studied systems the temperature of onset of magnetic hyperfine splitting is *depressed* relative to the 3D-antiferromagnetic ordering temperature in pure FeOCl. For this material we find (via Mössbauer spectroscopy) a value of $T_N = 85\ K \pm 1\ K$. The hyperfine splitting of the pristine material is indeed a sharp *ordering* with a highly temperature-dependent internal field. This contrasts strongly with the organosulfur systems, whose hyperfine splitting behavior corresponds to a gradual slow paramagnetic relaxation process. The intensity of the hyperfine pattern grows over a large temperature range as shown in Figure 8. In fact, the 78 K spectrum suggests the presence of more than one slowly relaxing environment in addition to the central rapidly relaxing paramagnetic phase doublet.

The observed "high temperature" slow paramagnetic relaxation is most probably due to the presence of the paramagnetic organosulfur radical cation, for which the spin density is relatively highly delocalized. This, together with the metal ion dilution effect raising from the bulk of the intercalant, leads to (a) a loss of the 3D order and (b) long spin–spin relaxation times.

Magnetic Susceptibility. The molar susceptibility of FeOCl and the intercalates between 5 and 300 K is shown in Figure 9. The room temperature magnetic moments per ion atom range from 2.76 μ_B for FeOCl to 2.8–2.9 μ_B for the intercalants; these values are substantially reduced from that expected for high-spin iron(III) (5.96 μ_B). These results are most readily interpreted in terms of strong antiferromagnetic coupling between the iron atoms.

Although a great deal of information on magnetic interactions in FeOCl and its intercalates has been obtained from Mössbauer spectroscopy,[14,35c,57,60,63-65] relatively few direct magnetic susceptibility results have been reported on these systems.[15b,66] Our results for FeOCl agree quite well with those of Halbert et al.,[15b] except that the low-temperature cusp reported by these authors at ca. 15 K is absent; these results do not agree with those of Bizette and Adam.[66] The most important feature is the lack of temperature dependence; as noted earlier,[15b] the susceptibility varies by less than 10% over the range 5–300 K. This behavior has been attributed to short range magnetic interactions that are

(65) Grant, R. W. *J. App. Phys.* **1971**, *42*, 1619–1620.
(66) Bizette, H.; Adam, A. *C. R. Acad. Sci. Paris* **1972**, *275*, 911–914.

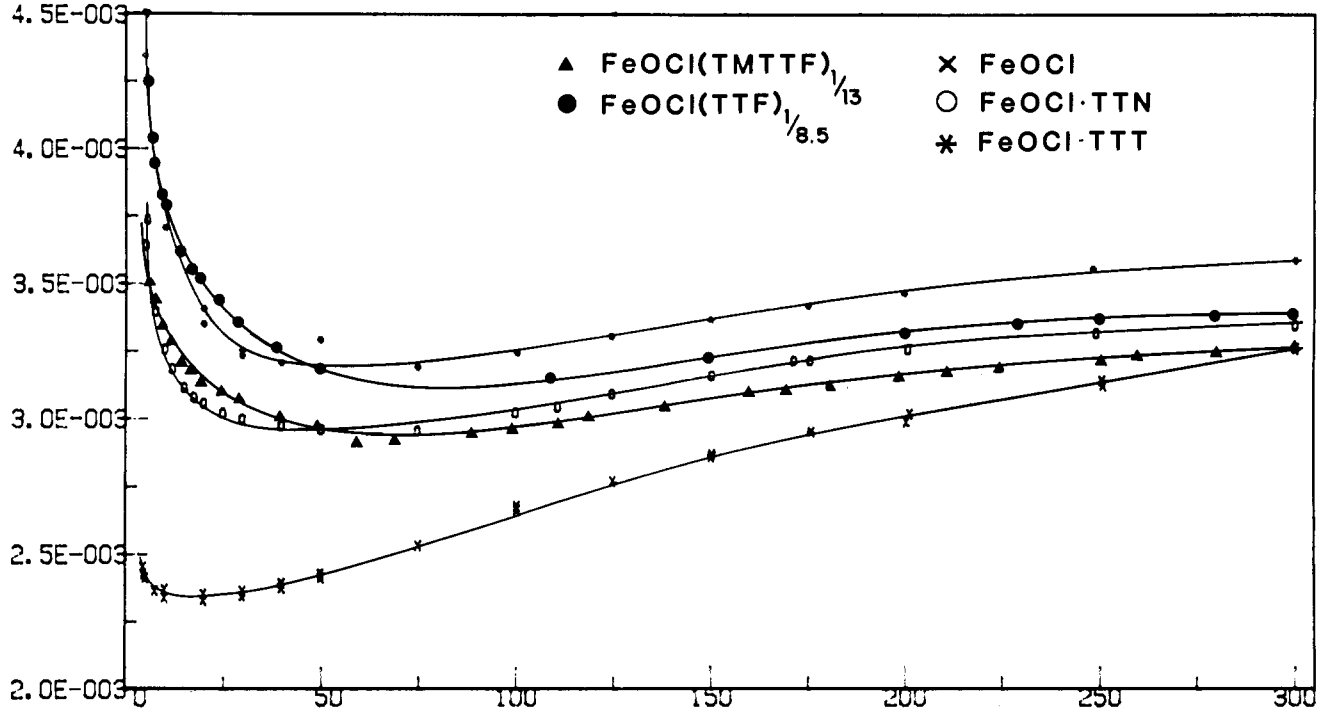

Figure 9. χ_m vs. T for FeOCl, $FeOCl(TMTTF)_{1/13}$, $FeOCl(TTF)_{1/8.5}$, $FeOCl(TTN)_{1/9}(tol)_{1/21}$, and $FeOCl(TTT)_{1/9}(tol)_{1/23}$ with lines drawn through the points.

fluctuating on a time scale faster than can be resolved by Mössbauer spectroscopy.

The variable temperature susceptibility data for the intercalates (Figure 9) are very similar to those of FeOCl. Except for a low-temperature Curie tail that may be due to paramagnetic impurities, the susceptibilities are almost temperature-independent between 90 and 300 K. The similarity of the susceptibility curves for FeOCl and the intercalates suggests that the short-range magnetic interactions observed in FeOCl are also present in the intercalates. The results for the tetrathiolene intercalates differ significantly from those reported for metallocene intercalates of FeOCl,[15b] for which a significant Curie contribution of undetermined origin was observed. Since vibrational spectra clearly indicate that the tetrathiolenes are present as the radical cations, relatively strong intermolecular interactions leading to pairing of the radical cation spins must be present in the intercalates. The lack of a Curie term for the tetrathiolene intercalates suggests that the electrons donated to the FeOCl host are not localized; this is consistent with the significant increases in electrical conductivity observed upon intercalation.

Further evidence for the lack of long-range magnetic ordering in the intercalates is provided by a recent low-temperature neutron diffraction study.[67] Neutron powder diffraction data measured at 10 K for FeOCl confirmed the magnetic lattice proposed by Adam and Buisson,[68] in which the crystallographic lattice is doubled along both the a and b axes, and the spins are rotated by 99° from one unit cell to the next along the c direction. Analogous low-temperature data for $FeOCl(TTF)_{1/8.5}$ showed no new peaks vs. room-temperature data, indicating that the 3D magnetic order present in FeOCl[68] is abolished upon intercalation. Since pristine FeOCl exhibits antiferromagnetic coupling along the b axis, it is not surprising that intercalation abolishes the 3D or long-range order.

Conclusion

Intercalation of organosulfur compounds such as TTF into FeOCl has resulted in formation of new low-dimensional materials. Infrared and Fe Mössbauer spectra confirm the existence of charge transfer from the tetrathiolene intercalant to the host. An absorption band due to an intervalence charge transfer could not be identified in the room temperature near-IR and optical spectra but may be obscured by the background absorption. The observed increase in conductivity of the intercalants over that of pristine FeOCl is attributed to injection of additional charges into the FeOCl layers, which provide the dominant pathway for electron transport. Although Fe Mössbauer spectra indicate only 4% and 6% Fe^{2+} in $FeOCl(TTF)_{1/8.5}$ and $FeOCl(TTN)_{1/9}$, respectively, there is no evidence for neutral intercalant molecules within the layers.

Long-range magnetic interactions within the FeOCl host lattice are affected by intercalation. The proposed magnetic lattice of FeOCl consists of Fe^{3+} antiferromagnetically coupled along the b axis, the interlayer axis. Upon intercalation this magnetic interaction is abolished by the expansion and doubling of the b axis. This is reflected in the magnetic susceptibility and neutron powder diffraction data.

Solid state wideline NMR spectra provide further insight into the orientation and interactions of the TTF molecule within FeOCl. The ^1H line shapes and hole-burning experiments can be most simply interpreted as evidence for molecular domains with different structural and/or dynamic characteristics. Further NMR studies are underway in order to obtain a better understanding of the dynamics of the organosulfur molecule within the FeOCl layers.

Current work in our laboratories is focused on intercalation of the selenium analogues of TTF and TTT and on developing methods for controlling the degree of charge transfer. This work will result in a more complete understanding of these systems, which will allow one to predict and to tailor the properties of these new materials to meet specific demands.

Acknowledgment. This research was supported by the National Science Foundation, Solid State Chemistry, Grant DMR-8313252 (S.M.K. and B.A.A.) and Grant DMR-8313710 (P.D.S. and W.J.R.). B.A.A. was an Alfred P. Sloan Fellow, 1981–85. We thank J. S. Frye for the CPMAS NMR spectra collected at the Colorado Regional NMR Center, NSF CHE-8208821, and J. L. Dye for use of the SQUID susceptometer.

Supplementary Material Available: Spectral parameters for NMR data and infrared spectra of the intercalates (7 pages). Ordering information is given on any current masthead page.

(67) Kauzlarich, S. M.; Faber, J., Jr.; Averill, B. A., unpublished research.
(68) Adam, A.; Buisson, G. *Phys. Status Solidi A* **1975**, *30*, 323–329.